Powder Filters for a Dilution Fridge Scanning Tunneling Microscope

by

Damien Charles Quentin

B.A.Sc., The University of British Columbia, 2012

A THESIS SUBMITTED IN PARTIAL FULFILLMENT OF
THE REQUIREMENTS FOR THE DEGREE OF

MASTER OF APPLIED SCIENCE

in

The Faculty of Graduate and Postdoctoral Studies

(Physics)

THE UNIVERSITY OF BRITISH COLUMBIA

(Vancouver)

March 2016

Abstract

In this thesis I present the design, construction, and characterization of metal powder microwave filters for a dilution refrigeration scanning tunneling microscope (STM) in the Laboratory for Atomic Imaging Research at the University of British Columbia. Scanning tunneling spectroscopy (STS) measurements performed by the STM are able to reveal features in the local density of states with energy resolution in the μeV regime if the sample and tunnel junction are cooled below 100 mK. The filters described in this work eliminate thermal noise and electromagnetic interference, which decrease energy resolution in STS measurements, up to seemingly indefinite frequency by exploiting the tremendous effective surface area of the metal powder which dissipates radio-frequency power via eddy currents induced in the grains.

Preface

The work presented in this thesis is unpublished, original, and independently performed by the author, D. Quentin.

Table of Contents

List of Tables

List of Figures

Chapter 1

Introduction

1.1 Scanning Tunneling Microscopy

Scanning tunneling microscopy (STM) is a tool that can provide atomic topographic images and electronic characterization of exciting new materials. The topographic images produced are real-space 2-dimensional images obtained by approaching a very fine tip to within a few nanometers of a sample in ultra-high vacuum (UHV), and applying a voltage potential across the junction. The tip and sample are so close the wavefunctions of the electrons in the tip and sample overlap, allowing electrons to tunnel across the junction when a voltage is applied.

Since the tunneling current depends exponentially on gap distance with decay length $\hbar(8m\phi)^{-1/2}$, topographic images can be well-resolved at the atomic scale by two separate techniques: constant-current or constant-height imaging. In constant-current mode, the feedback control system adjusts the tip-sample separation distance to keep the tunneling current constant as the tip scans over the surface of the sample. Scanning speed in this mode is limited by the feedback bandwidth. In constant-height mode, the tip-sample separation distance is held constant while the current is directly measured. This method is limited to fairly flat sample surfaces to keep the tip from crashing into the sample, though since there is no feedback the scanning speed can be faster.

In addition to topographic images, spectroscopic images can be produced using the same instrumentation with a method called scanning tunneling spectroscopy (STS), whereby the tip is still scanned over the sample but at each pixel in the array, the tip is held in position while the bias is swept across a range of voltages to extract a tunneling conductance, dI/dV, either by differentiation or by adding a small AC modulation. dI/dV is a very useful quantity to extract since it relates to the local density of states (LDOS), which is useful in exploring many physical phenomena.

1.2 UBC LAIR Facility and Instrumentation

The Laboratory for Atomic Imaging Research (LAIR) facility at UBC consists of 3 different STM's housed in separately isolated rooms. Due to the exponential dependence of tunneling current on tip-sample separation, having an environment with minimal vibrations is essential. The STM rooms have a separate foundation from the rest of the building; they don't share any walls, ceilings, or floor space with the rest of the building and are only coupled through the earth. This allows for the best possible vibration isolation. To further isolate the experiments from vibrations, the microscopes are mounted on massive inertial concrete slabs, which themselves are mounted on pneumatic isolators. The dilution fridge STM, which is the system of focus in this thesis, is mounted on a 70-tonne concrete slab, the largest of the three in the LAIR.

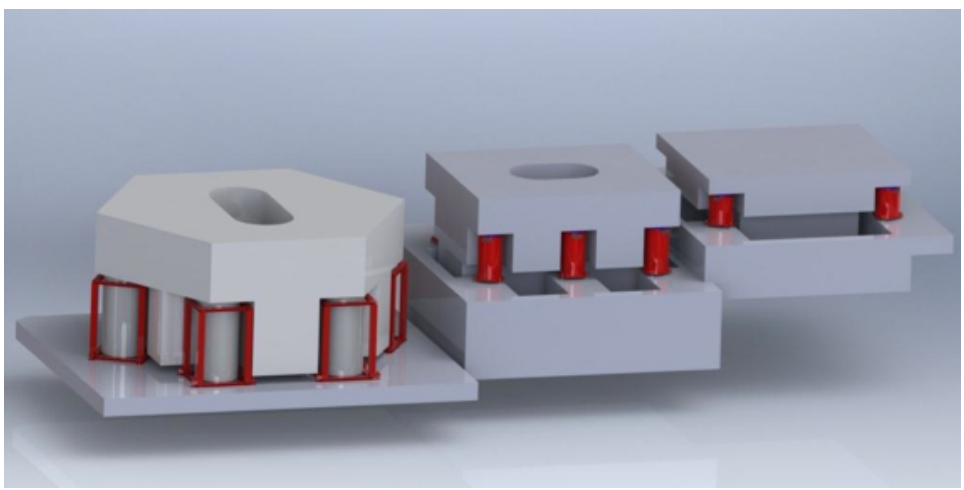

Figure 1.1: STM inertial slabs (reprinted with permission of Prof. Doug Bonn) [1]

In addition to the slabs being mounted on large pneumatic isolators, the aluminum frames supporting the individual UHV systems are themselves mounted on smaller pneumatic isolators atop the slabs. Along with acoustic damping pads hanging from the walls, the end result is a low and stable tunneling noise floor, and an eerie silence in the rooms with the doors closed tightly.

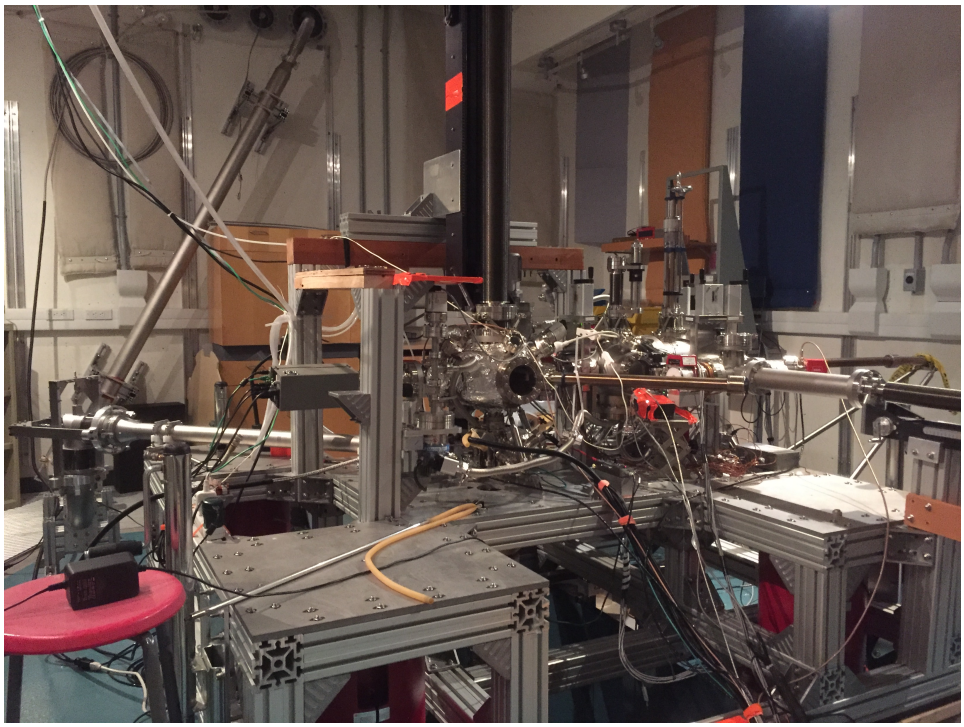

Figure 1.2: Dilution fridge STM in the Laboratory for Atomic Imaging Research

The ^{3}He - ^{4}He dilution fridge is built by Janis Research Company, model JDR-50-UHV-STM. The fridge base temperature is 35 mK. The vector magnets are fixed within the liquid helium dewar, which has a belly capacity of 65 liters and a boil-off rate of 250-350 cc/hour. The maximum vertical magnetic field is 7 Tesla at 4.2 K, and the maximum horizontal field is 2 Tesla at 4.2 K. With both coils running simultaneously the maximum field is 1 Tesla at 4.2 K.

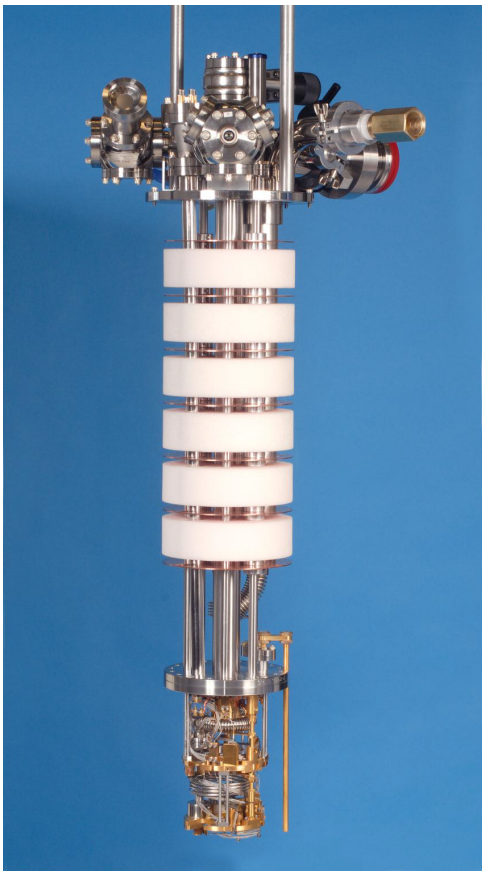

Figure 1.3: Dilution refrigerator (image courtesy of Janis Research Company)

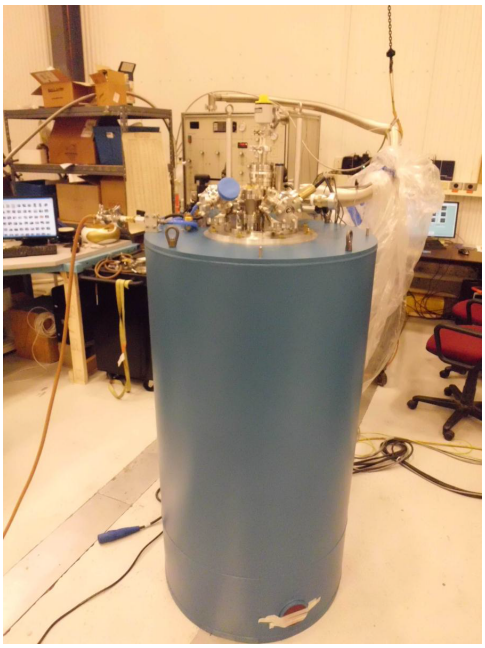

Figure 1.4: Liquid helium dewar for dilution fridge system (image courtesy of Janis Research Systems)

1.3 The Problem with Noise

All wires, to some extent, behave as antennas. A deliberately-designed antenna will transmit, and pick up, certain frequencies better than others, but any arrangement of wires will still transmit or receive electromagnetic radiation. This pick-up is called electromagnetic interference (EMI), and in general, careful design considerations such as keeping wires short and avoiding loops can greatly reduce this interference and is often sufficient.

The dilution fridge STM at the UBC LAIR is located in a low-vibration facility, with all instrumentation and control electronics kept in a corridor outside. As such, all wires leading into the UHV system are 20 to 50 feet long. Since the wire carrying the tunneling current is connected to an amplifier with 10^9 gain, EMI can have a tremendous impact and poses a significant problem. For instance, AC adapters plugged into power outlets near any wires introduce 60Hz noise peaks several orders of magnitude higher than the noise floor.

In addition to EMI, a significant source of noise is Johnson noise. John-

son noise (sometimes called thermal noise or Nyquist noise) is electronic noise created by thermal fluctuations of electrons. This noise is present in any dissipative element.

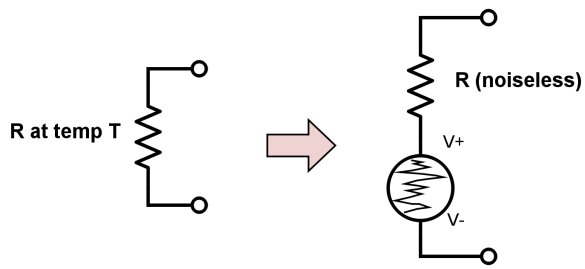

Figure 1.5: Equivalent circuit for a resistance at a temperature T

The noise voltage can be expressed as $\bar{e}_n^2 = 4k_BTR\Delta f$, where k_B is Boltzmann's constant in Joules per Kelvin, T is the temperature in degrees Kelvin, R is the resistance in Ohms, and Δf is the bandwidth in Hertz over which the noise is measured. As a rule of thumb to provide some intuition, 50 Ω at room temperature produces approximately 1 nV/$\sqrt{\text{Hz}}$. For the vast majority of electronic systems, this level of noise is not a concern, but in low temperature physics experiments where the signals are typically minuscule, Johnson noise can have a relatively large presence and should always be accounted for. At 300 K, Johnson noise radiation peaks at roughly 6 THz [2].

In STM, noise increases electronic temperature. The noisy fluctuations of the electrons give the illusion the system is at a higher temperature than it actually is (base temperature). This increase in electronic temperature could easily be on the order of a few Kelvin. This can be most easily seen in conductance plots taken by STS, where the thermal broadening causes a decrease in energy resolution. Certain features such as Zeeman or hyperfine splitting can only be seen in the LDOS at very high energy resolution [3], which is why these experiments are run in the 10's of milliKelvin regime with dilution refrigeration systems.

Aside from proper shielding and design configuration, the best way to mitigate noise is to install filters. Since the cables and wires are near enough to each other that they are capacitively coupled, and since the inside of the steel UHV system behaves to a certain degree like a microwave cavity, it's crucial to filter each and every wire entering the microscope. Given that Johnson noise extends into the terahertz regime, special considerations need

to be made in the design of the filters that allow them to maintain high attenuation at these frequencies.

1.4 Powder Filters

The vast majority of electronic filters used today are active filters. These are filters which use an amplifier to keep the filters small, inexpensive, and easy to manufacture on a large scale. However, amplifiers have very large resistances, typically on the order of 10^6 Ω. This poses a problem for sensitive low-temperature physics experiments as these filters add considerable Johnson noise. It is therefore necessary to use passive filters (those without amplifiers or an external power source) as they can be made with very low resistance.

In 1987, Martinis et al. used metal powder to create a passive filter whose attenuation increases with frequency seemingly indefinitely [4]. The filters consisted of an insulated Manganin coil inside a copper tube filled with 30 μm grain copper powder. The filter was 0.1 m long, and they measured an attenuation of more than 50 dB from 0.5–12 GHz. This filter provides attenuation via two separate mechanisms. First, it is clear from the impedance of the inductor, $Z_L = j\omega L$, that as the frequency ω increases, so does the impedance until eventually it is so high the inductor starts to behave as an open circuit. However, there is a problem which all inductors have at very high frequencies. Neighbouring windings are separated by a thin layer of insulation; this forms a small interwinding capacitance, and beyond a certain frequency the inductor will behave as a short circuit as the higher frequencies essentially bypass each loop. Thus, at very high frequencies inductors become ineffective. The Martinis filter's second mechanism of attenuation combats this issue, and is what makes this filter special.

The effectively massive surface area of the copper powder, whose grains are insulated by a naturally-grown oxide layer, allows for eddy currents induced in the powder to greatly attenuate higher frequencies via the skin effect. The skin effect is the frequency-dependent tendency for current to be distributed near the edge of a conductor. The AC current density decays from the surface exponentially inside the conductor with decay length $\delta = \sqrt{\frac{2\rho}{\omega\mu}}\sqrt{\sqrt{1+(\rho\omega\epsilon)^2}+\rho\omega\epsilon}$, where ρ is the conductor resistivity, ω is the angular frequency of the current, and μ and ϵ are the permeability and permittivity of the conductor, respectively. We call δ the *skin depth*. With the current condensed at the conductor edges, the conductor's resistance is effectively increased at higher frequencies, allowing greater dissipation of RF

power.

In 2008, Lukashenko and Ustinov [5] improved upon the design of the Martinis powder filter by adding capacitors to make the filter an LC-Π powder filter, so-called because the circuit diagram looks like the Greek letter Π. LC-Π filters are low-pass filters consisting of a series inductance with capacitors to ground at both the input and output. They are a convenient type of filter because they have inherently low impedance, a very flat passband response, and their circuit diagram is very simple. Again, their use in practice is limited due to the cost of implementing inductors.

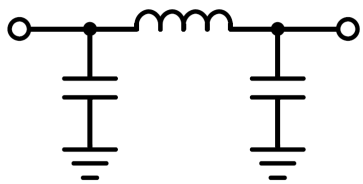

Figure 1.6: Circuit diagram of an LC-Π filter

In addition to introducing capacitors, Lukashenko and Ustinov further improved the Martinis design by using stainless steel powder instead of copper powder, since the resistivity of stainless steel is nearly an order of magnitude higher than that of copper. As a result, these filters have a cutoff frequency of 1 MHz, a rolloff of -50 dB per decade, and hit the noise floor (-100 dB) around 200 MHz.

Where magnetic fields and magnetization are not concerns, stainless steel is a common choice for metal powder. However, if the filters are well away from sensitive systems and magnetic fields, iron powder is sometimes a better alternative. Due to its high relative magnetic permeability, adding iron powder to an inductor increases the inductance since inductance is linearly proportional to permeability.

1.5 Overview

In this thesis I describe the theory, construction, and characterization of an LC-Π metal powder filter system for use in a dilution refrigeration UHV STM in the Laboratory for Atomic Imaging Research (LAIR) at the University of British Columbia (UBC).

I begin by discussing the details of the design of the LC-Π powder filters,

the housing assemblies, and the conduits. I then discuss special design considerations for the different components of the STM system, and how this affects the designs of the filtering system. Following that I provide a detailed summary of the construction and assembly procedure for the different filters and components in the filtering system. Finally, I characterize performance and present attenuation data for all filters in the system.

Chapter 2

System Details and Design Considerations

When designing the filtering system it's crucial to consider the requirements of each of the lines to be filtered. It's necessary to know the required bandwidth, impedances, and capacitances to ensure the filters wouldn't alter the data or signals on each of the wires entering the system.

2.1 UHV Wiring

Below is a wiring diagram for the dilution fridge provided by Janis Research Company. The diagram is useful in outlining how and where lines are connected at the various stages of the system. Details on the wiring of components other than those supplied by Janis are shown in tables in this section, along with pin assignments for the filter assembly connectors.

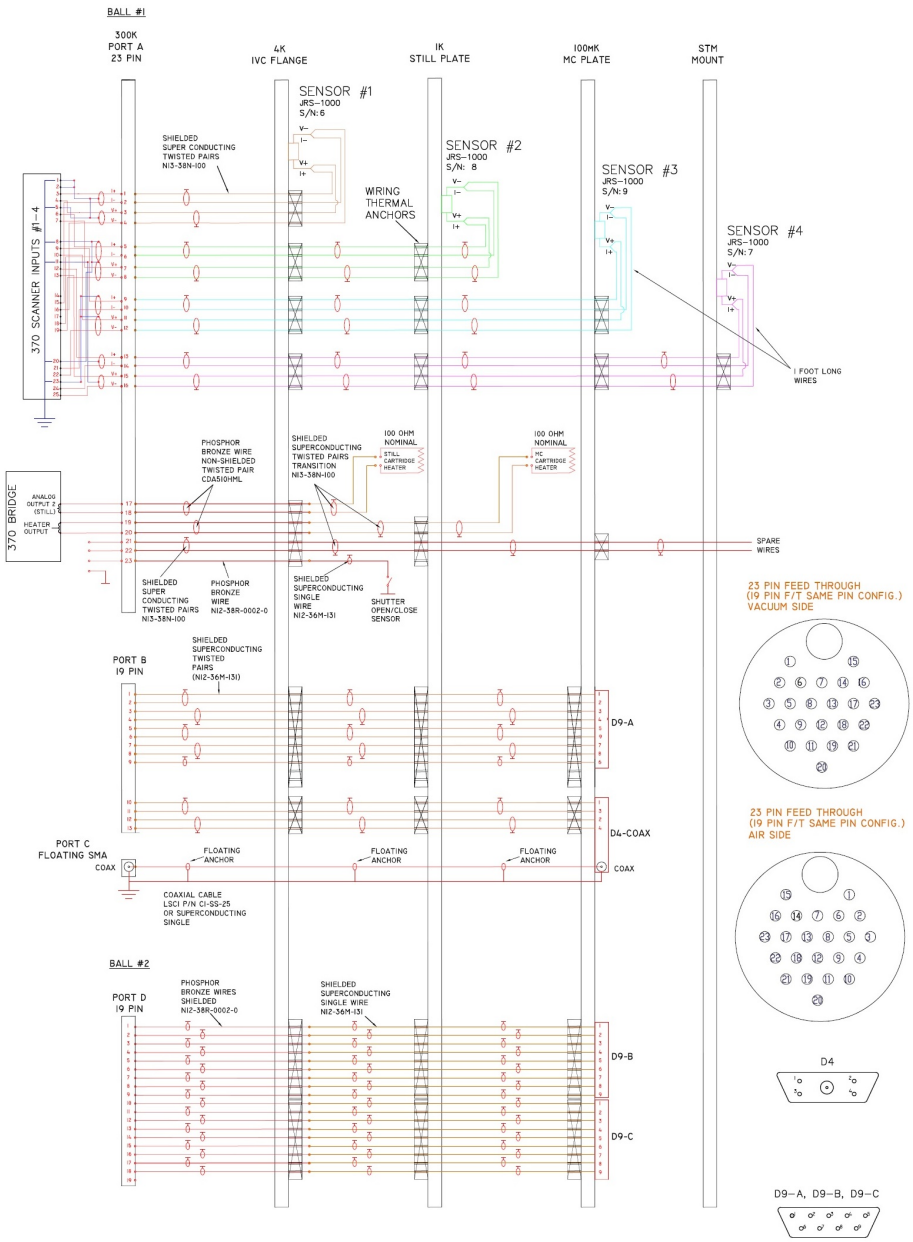

Figure 2.1: UHV wiring diagram (image courtesy of Janis Research Systems)

There is an adapter on Port A to convert between a 23-pin Delrin sub-C

Device	Port Pin	MIL. Pin	Bridge Pin
Janis Thermometer 1: I+	1	R	3
Janis Thermometer 1: I-	2	S	15
Janis Thermometer 1: V+	3	Z	4
Janis Thermometer 1: V-	4	Y	16
Janis Thermometer 2: I+	5	T	6
Janis Thermometer 2: I-	6	P	18
Janis Thermometer 2: V+	7	G	7
Janis Thermometer 2: V-	8	N	19
Janis Thermometer 3: I+	9	U	9
Janis Thermometer 3: I-	10	X	21
Janis Thermometer 3: V+	11	V	10
Janis Thermometer 3: V-	12	M	22
Janis Thermometer 4: I+	13	H	12
Janis Thermometer 4: I-	14	F	24
Janis Thermometer 4: V+	15	A	13
Janis Thermometer 4: V-	16	B	25
Still Cartridge Heater	17	E	
Still Cartridge Heater	18	J	
MC Cartridge Heater	19	L	
MC Cartridge Heater	20	W	
No Pin	21		
No Pin	22		
Shutter Sensor	23	C	

Table 2.1: Electrical pinouts for UHV wiring port A

connector to a MIL MS3476L14-23S connector. Table 2.1 shows the corresponding pins on the MIL connector and the pins on the Lakeshore Resistance Bridge.

Device	Pin
Y- Scanner	A
Bias (East)	B
X- Scanner	C
X+ Scanner	D
Capacitive Sensor (Bottom)	E
RuO_2 Sensor	F
Bias (West)	G
Y+ Scanner	M
RuO_2 Sensor	N
Capacitive Sensor (Inner)	P
Capacitive Sensor (Top)	R
RuO_2 Sensor	S
RuO_2 Sensor	V

Table 2.2: Electrical pinouts for UHV wiring port B

Device	Pin
Slip Stick Stack IV-	A
Position Sensor	B
Slip Stick Stack VI+	C
Slip Stick Stack IV+	D
RuO_2 Sensor	E
Slip Stick Stack I-	F
Slip Stick Stack III-	G
RuO_2 Sensor	H
Slip Stick Stack V+	J
Slip Stick Stack III+	K
Slip Stick Stack I+	L
Sample Input	M
RuO_2 Sensor	N
Slip Stick Stack VI-	P
Sample Input	R
Slip Stick Stack II+	S
Slip Stick Stack V-	T
Slip Stick Stack II-	U
Z Scanner	V

Table 2.3: Electrical pinouts for UHV wiring port D

2.2 Design Considerations

Tunneling Current

The tunneling signal has a low bandwidth and low current. The only special consideration to be made in designing the tunneling filter is the large impedance of the tunnel junction. The impedance of the tunnel junction is typically on the order of 10^9 Ω, so it's important that the filter impedance to ground be large to avoid losing significant current.

Coarse Position Control

The sample is brought into the STM head by servo-motor control of a vertical arm which holds the sample and sample plate, but once the sample is within about a centimeter of the probe tip, the tip is approached to the sample by shear stack piezoelectric actuators. We refer to this as *coarse position control*, though in this context since the actuator resolution is roughly 100 nm, *coarse* is somewhat of a misnomer—so-called because finer positioning control (less than 0.1 nm) is performed by a separate mechanism to be discussed in the next section.

The coarse approach is performed by (relatively) slowly ramping the voltage to the piezoelectric stacks and then very rapidly grounding them. With one side of the stack fixed to the Macor head and the other side simply pressed up against the prism (to which the tip is mounted), shearing the stack has the effect of moving the prism up or down; however, if the voltage applied to the stack returns to 0 quickly enough, the stack will slip along the surface of the prism, leaving the prism in its new position. For this reason, this type of actuator is sometimes referred to as a *stick-slip actuator*.

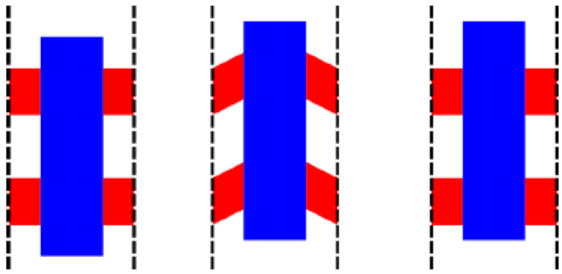

Figure 2.2: The coarse approach piezoelectric actuators shear under an applied bias, then snap back into position to move the STM tip [6].

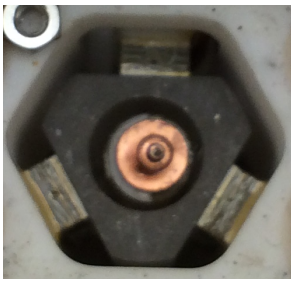

Figure 2.3: The sapphire prism which holds the STM tip is supported by a set of 3 shear stack piezoelectric actuators (image courtesy of Robert Delaney).

The shape of the waveform driving the stack of piezoelectric actuators is crucial to proper stick-slip action, and if a filter alters this shape too much the actuators may not work properly. The max slew rate for the driver output is 500 MV/s at 2A for 1 μs, 300 times per second. To avoid altering the shape of the waveform, a filter with a higher cutoff frequency is preferred. Additionally, NiCr wire would be avoided for this application. NiCr is resistive wire which would lower the cutoff frequency but in addition, the dissipated power would provide roughly 1 W of heat. Even though this is a relatively small amount, heating can be problematic since iron powder sinters easily. Sintered powder would form a resistive path to ground within the filter, reducing the voltage delivered.

Fine Position Control

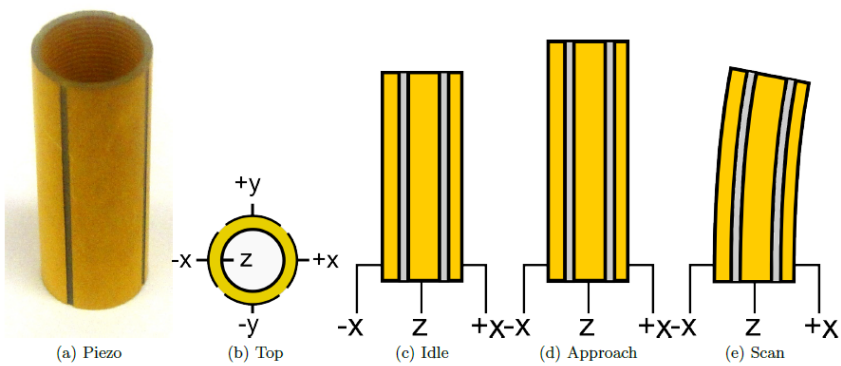

(a) Piezo (b) Top (c) Idle (d) Approach (e) Scan

Figure 2.4: The PZT tube allows for lateral and vertical fine position control [6]

Fine control of the tip is achieved by a PZT tube with an arrangement of contacts that allows for deflection, elongation, and deformation of the tube. Four evenly-spaced contacts on the outside of the tube allow for lateral control by shearing the tube, and a contact along the inside of the tube allows the entire tube to be elongated and compressed.

In order to deform the tube to desired lengths and shapes, the maximum voltage applied to the PZT is 220V. This voltage is high enough to cause a breakdown of the dielectric in the metal powder grains, so the wire must be particularly well-insulated.

When there is a breakdown of the dielectric and enough current flows to ground, not only is the piezo tube not able to maintain the desired position, but the lost current is picked up by the tunneling amplifier which raises the noise floor by orders of magnitude.

Cold Bias Filter

Due to space constraints, every line into the system is filtered at room temperature instead of in the UHV space. However, there is still room for some filtering in UHV on the STM head, so a single filter is installed on the bias line.

Since the bias line has a high impedance and very low bandwidth, there are no special *electronic* design constraints; however, making

components for UHV requires special care. Most of the metal used in the filter should be gold-plated oxygen-free high thermal conductivity (OFHC) copper. OFHC copper is used instead of regular copper because of its higher thermal conductivity and low relative volitility (it out-gasses easily), and should be gold-plated to avoid problems with oxidization. Additionally, to avoid contaminating the vacuum, all internal components should be fully potted in Epo-Tek H77 Epoxy, which is electrically insulating and thermally conductive.

Thermometry

A number of thermometers are placed throughout the dilution fridge system. Temperature measurements are done by 4-wire lock-in measurements of RuO_2 chips, whose resistance provides an accurate measure of temperature, particularly at low temperatures.

Placing an LC-Π filter on these lines adds a capacitance in parallel to the RuO_2 chips, and since the lock-in amplifier drives the measurements at 13 Hz, it's worth considering the impedance of the capacitor to ensure there is no significant current flowing through the capacitor.

To provide a reference, consider the case where the impedance of the capacitor is equal to that of the RuO_2 thermometer, which can reach a megaohm when the dilution fridge is running. In this case, equal current would flow through the capacitors as through the thermometer chips. The capacitance required to achieve such an impedance would be

$$C = \frac{1}{2\pi \times 13{\times}10^6} = 10^4 \text{ pF} \tag{2.1}$$

10^4 pF is a fairly large capacitance, and it is easy to keep the filter capacitance orders of magnitude below this level.

Magnetic Field

The presence of a strong magnetic field can alter the attenuation characteristics of the powder filters by saturating the field within the inductors.

According to magnetic field profiles provided by the system's magnet manufacturer, American Magnetics, Inc., with the superconducting magnets operating at full strength, the room-temperature filters placed 1.5–2 m away from the magnets would see a maximum of approximately 100 Gauss. This is a relatively small value, as B-H curves

of similar iron powder show that 100 Gauss is still well within the linear regime.

Chapter 3

Construction and Assembly

The following are sets of instructions to make and prepare the filters and assemblies used in this system.

3.1 Powder Filters

1. Making the inductor cores begins by mixing a batch of Stycast 1266 epoxy with -325 mesh iron metal powder, 50/50 by weight. Stycast 1266 is a good epoxy to use because it has a fairly low viscosity and high resistivity.

2. De-gas the epoxy by placing the mixture in a low-pressure chamber. Do this until most of the bubbling has subsided. Placing the epoxy in low pressure for too long will evaporate some of the epoxy constituents and will prevent it from curing properly.

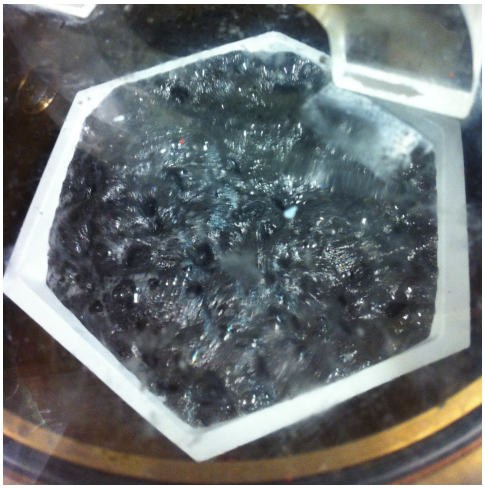

Figure 3.1: Air violently escaping the epoxy/powder mixture in a low-pressure chamber

3. Use a teflon tube with 1/8" inner diameter connected to a vacuum pump as a mold to cast the epoxy/powder mixture. To contain the mixture during the cure, plug the top of the teflon tube with a small amount of Blu-Tack putty.

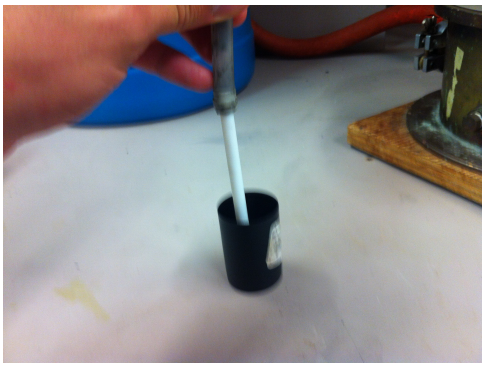

Figure 3.2: Use a vacuum pump connected to a vinyl hose to suck the epoxy mixture into a teflon tube.

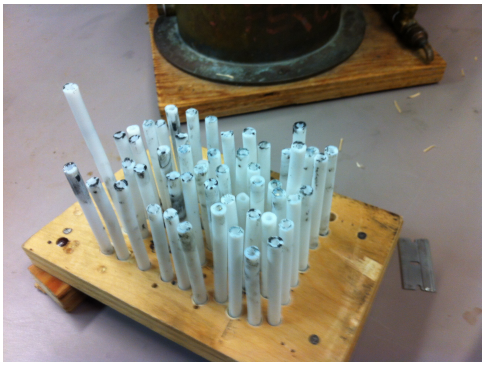

Figure 3.3: Cure the inductor cores using teflon tubes as molds.

4. Teflon is a good material to use because the epoxy doesn't stick to it, and if the epoxy cores are tough to extract, the tubes will expand when heated. The easiest way to extract the cores is to hammer a 1/8" brass rod down the teflon tube and push the cores out the bottom.

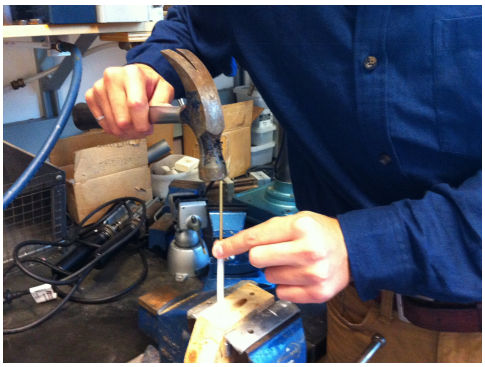

Figure 3.4: Hammer a 1/8" rod through the teflon tubes to extract the inductor cores.

Figure 3.5: 3 cm-long inductor cores.

5. Once extracted, cut the cores into 3-cm lengths. One by one, place the cores in a lathe to bore 3-mm-deep holes into the ends using a size 55 drill bit. These holes will ultimately hold the inductor pins.

6. Use a jig to wind the inductor about the cores. A good wire to use is 0.0031" NiCr enameled wire with a resistance of 81.09 Ω/ft manufactured by Evanohm. With this wire, each inductor consists of roughly 8.5' of wire for an average resistance around 700 Ω. Once the inductors are fully wound, apply 5-minute epoxy to the windings to hold them in place.

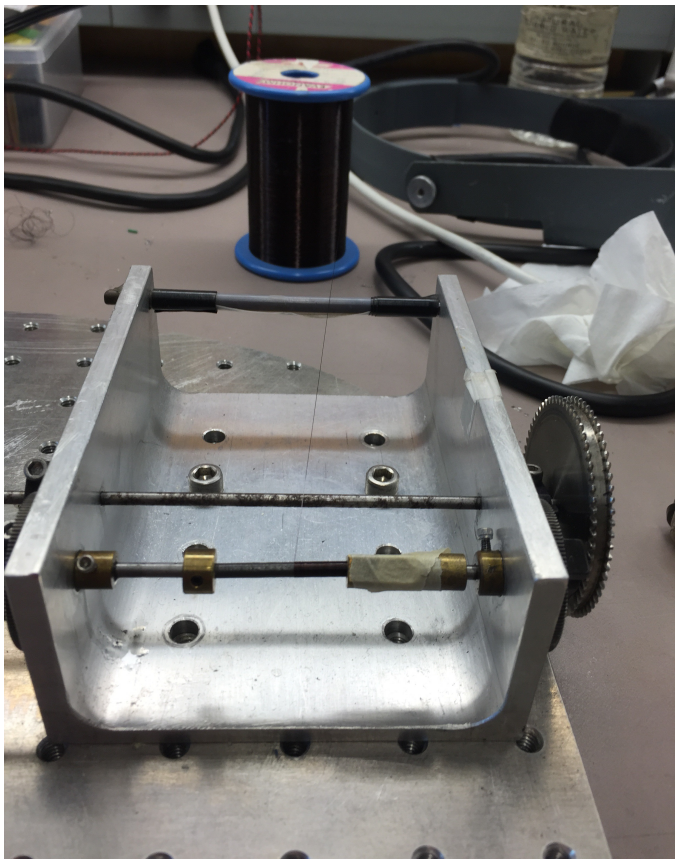

Figure 3.6: Winding jig for the inductor cores.

7. With the windings fixed in place by epoxy, install the pins on each inductor. Straighten 2-cm sections of 16 AWG tinned bus wire (this is very easy to straighten perfectly by clamping one end of the wire in a vise, and then using pliers to pull on the other end until the wire yields and stretches). In order to ensure a tight fit of the pins in the inductor cores, gently flatten one of the ends of the wire with a hammer to slightly increase its diameter, then coat it with 5-minute epoxy before finally placing the pins in the inductor core holes.

Figure 3.7: Inductor with pins installed and one end soldered.

8. The next step is to solder the NiCr wire to the inductor pins. This step is quite challenging, and great care must be taken not to melt the epoxies, which starts to happen around 100 °C. Therefore, the soldering should be done quickly.

   (a) Strip the enamel from one of the loose wire ends using a razor blade. Be careful not to unwind the inductor or to knick the wire.

   (b) Ensure a good bond by roughing the pin with sandpaper or a razor to increase surface area.

   (c) Wrap the free wire around the pin 3 or 4 times to ensure plenty of contact. Increase the strength of the joint by separating consecutive windings by roughly 0.5 mm. Use a jig to hold the wire tight and apply one or two drops of strong, corrosive acid flux.

   (d) Apply heat with the soldering iron while simultaneously holding a small piece of solid-core Pb-Sn solder until it wicks onto the pin windings.

   (e) Once all the free wires are soldered to the inductor pins, the assemblies must be thoroughly rinsed and cleaned with warm water in an ultra-sonic bath to avoid corrosion of the wires by the acid flux.

9. The next step is to solder a feed-through capacitor to one end of the inductors and then to mount the assembly within a tube. The capacitor I used is the Tusonix 2482-0120-X5U0-101MLF. It is 100 pF $\pm$ 20% with inner diameter 1.22 mm and outer diameter 4.95 $\pm$ 0.38 mm. It is very easy to solder these together as both surfaces are already tinned.

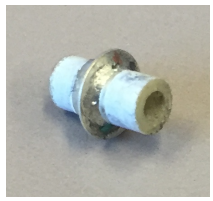

Figure 3.8: Feed-through capacitor used in the powder filters

Figure 3.9: First capacitor soldered to inductor

10. Prepare the filter outer conductor by cutting a 4 cm section of brass tubing, with inner diameter 7/32" and wall thickness of 0.014". Insert the inductor/capacitor assembly into the tube, and solder them together where the capacitor's outer contact meets the brass tubing. This capacitor will nest nicely in the tubing if you shave a small amount of brass from the inner wall using a reamer or de-burring tool.

11. Once the soldering is complete, all the extra flux has to be washed away in an unltrasonic bath or the corrosion will cause problems in the future. Even fairly non-corrosive flux such as rosin flux causes a problem; the fumes from the flux will permeate the powder within the filter and strip the oxide layer slowly. After a few months, the resistance parallel to the capacitor will decrease by several orders of magnitude, into the kiloohm regime.

Figure 3.10: Open assembly with a single capacitor

12. Next, fill the assembly with -325 mesh iron powder. To completely fill the space within the assembly, an effective technique is to hold the assembly upright to fill with powder, and periodically hold the assembly against something that vibrates so all the powder can settle to the bottom of the tube. A Dremel hand drill with a vinyl screw works quite well without causing any damage.

Figure 3.11: Settling the powder to the bottom of the inside of the assembly with a Dremel

13. Since iron powder tends to sinter rather easily and since there would be no way to clean any stray flux inside the filter, the second capacitor must not be soldered in place. Use a conductive epoxy that cures

at room temperature. Conductive epoxy that cures at higher temperatures must be avoided or the powder will sinter when heated. If the powder sinters, the resistance to ground will drop to the kiloohm regime.

14. Once the conductive epoxy has cured, all excess solder and epoxy must be removed so the outside of the tube is smooth. Otherwise the filters won't fit into the filter housing assembly.

Figure 3.12: A fully assembled powder filter

Figure 3.13: Cross section view of the LC-Π powder filter, to scale. For clarity, the powder is not shown. Also note that the windings may be too small to see.

3.2 Coarse Approach Filters

As discussed in the previous chapter, the filters for the coarse approach piezo lines need a higher cutoff frequency than the powder filters. We found that a low cutoff frequency deformed the waveform too much.

1. To allow for higher currents, the wire used in these inductors is 18 AWG enameled copper wire. Since this wire is much more rigid than the NiCr wire used in the powder filters in the previous section, these inductors don't need to be fixed to an epoxy/powder core. Instead, the windings are formed around a 1/8" brass rod and maintain their shape when slipped off. Once the coils are removed from the rod, carefully bend the free ends to run along the axis of the inductor, as shown in the figure below.

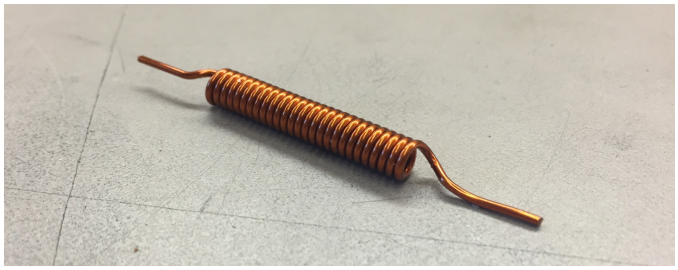

Figure 3.14: Inductor coil used in the coarse approach filters

2. Cut a 4 cm-long section of brass tubing with 3/8" outer diameter and 5/16" inner diameter to form the filter's outer conductor.

3. Place a section of 5/16" teflon rod in a lathe, and drill a hole several millimeters deep along the center with a size 58 drill bit.

4. With a razor blade, slice two disks off the rod, roughly 0.5 mm thick.

5. Work one of the teflon disks into one of the brass tube ends. Seal it in place with some 5-minute epoxy.

6. Insert the inductor in the brass tube and slide the end through the hole in the teflon disk. Use 5-minute epoxy to seal the pin in place.

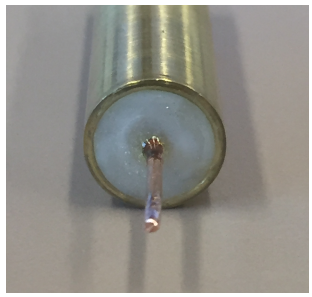

Figure 3.15: Teflon endpiece on coarse approach filter

7. Fill the tube with stainless steel powder.
8. Work the second teflon disk in place and seal it with 5-minute epoxy to retain all the powder.

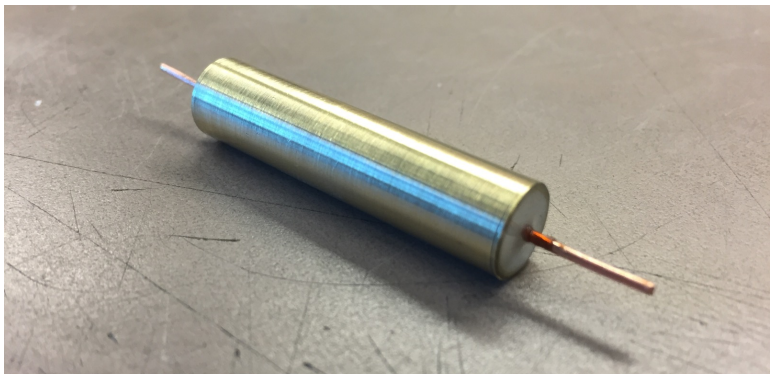

Figure 3.16: A fully assembled coarse approach filter

3.3 Cold Bias Filter

A single filter is installed on the phosphor-bronze stand-off—which connects the STM head to the mixing chamber—to filter the bias line at low temperatures. At millikelvin temperatures the Johnson noise produced by this filter would be significantly smaller than the room temperature equivalent.

To fix the head filter to the stand-off, a custom casing had to be machined.

1. Place a rod of OFHC copper, at least 1 cm in diamater, in a lathe. Bore a hole with a 6 mm drill bit to a depth of 45 mm.

2. Turn down a 45 mm section to a diameter of 8.5 mm.
3. Use a cutting tool to cut off a 40 mm-long section of the OFHC tube.

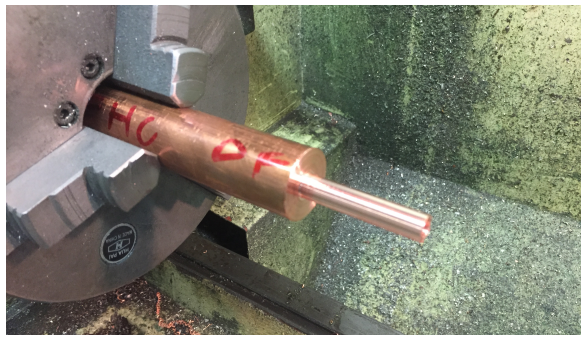

Figure 3.17: OFHC material in a lathe

4. Use a milling machine to mill a 3 mm-wide flat edge along the length of the tube.
5. Cut and drill a thin OFHC plate 60 mm x 12 mm with 4 M3 through-holes. These holes allow the filter assembly to be mounted directly onto the stand-off

Figure 3.18: OFHC plate to mount filter to STM head

6. Electroplate gold onto the OFHC pieces.

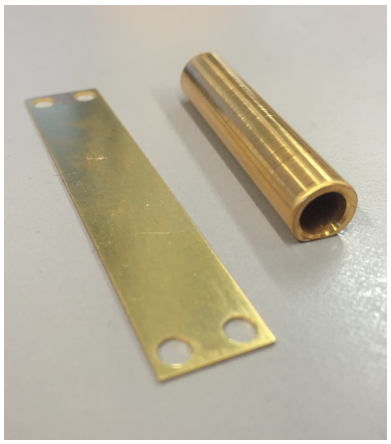

Figure 3.19: Gold-plated filter tube and mounting plate

7. Prepare the inductors in exactly the same was as was described for the LC-Π powder filters (with NiCr wire and epoxy/powder cores), however, use 316 stainless steel powder instead of iron since the filter will be exposed to strong magnetic fields.

8. Pot the inductor in the gold-plated tubing with a 50-50 mixture of Epo-Tek H77 epoxy and 316 stainless steel. Begin by preparing the mixture.

9. Plug one end of the tube with a thin slice of teflon, with a hole in the centre for the inductor pin to pass through. Do this in a similar way as was described in the coarse approach filter section, but do not use any epoxy to seal the teflon in place.

10. Place the assembly in a vise and a simple jig to keep it upright, and fill the tube with the mixture.

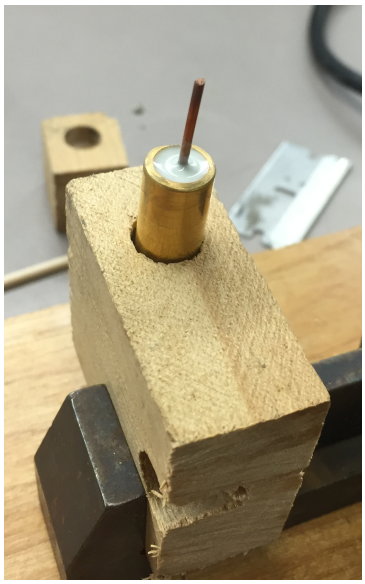

Figure 3.20: Jig for curing the epoxy/powder potting mixture in the cold bias filter assembly

11. Place assembly in 150 °C oven for a minimum of 1 hour to cure the epoxy.
12. Use a pick to gently remove the teflon disk.

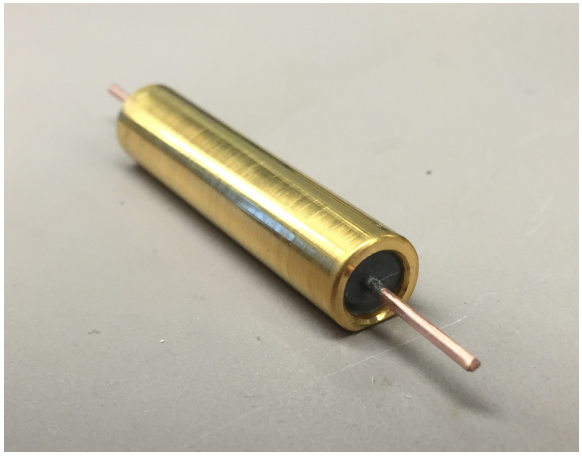

Figure 3.21: Potted filter tube with inductor.

13. Use Epo-Tek H20E silver epoxy to fix the filter tube to the mounting plate.

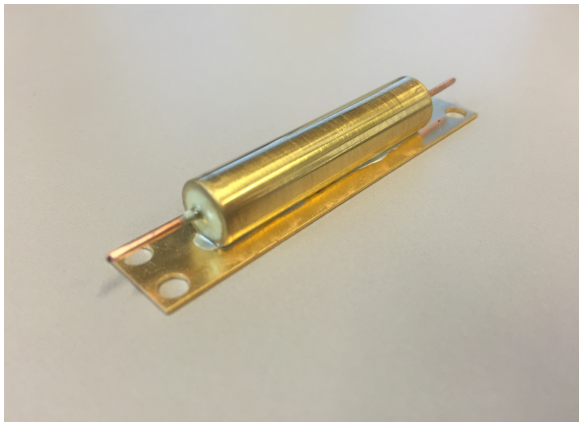

Figure 3.22: Completed head mount filter

3.4 Tunneling Filter

The tunneling line filter is very similar to the LC-Π powder filters, except that it has SMA connectors mounted directly to the filter instead of being mounted in a larger housing.

1. Prepare the inductor the same way as for the LC-Π powder filters, again using iron powder.
2. Cut the inductor pins so they are 5 mm long.
3. Slide the discoidal capacitors over the inductor pins all the way to the NiCr solder joint. Use acid flux and be very quick when soldering the capacitor to avoid melting the solder on the NiCr joint.

Figure 3.23: 100 pF capacitor for tunneling line filters, measuring approximately 3.5 mm in diameter. The part no. is INSTEC 140X101PC039

4. Cut a 44 cm-long section of 7/32” outer diameter brass tubing.

5. Bore a 1/8” hole in the side of the tubing, large enough to pour powder through.
6. Cut a small brass sleeve that can just slide over the 44-cm brass tubing long enough to completely cover the 1/8” hole.
7. The discoidal capacitor outer diameter is slightly smaller than the brass tubing inner diameter, so cut a short section of thin-walled brass tubing so that the capacitor can be connected to the outer conductor’s inside wall.
8. Use room-temperature conducting epoxy to attach the small thin-walled sleeve to the discoidal capacitor and the inside of the brass outer conductor.
9. Use room-temperature conducting epoxy to attach the SMA connector male and female pins to the inductor pins.
10. Insert one of the pins into the corresponding SMA connector dielectric.
11. With the SMA connector held in place, slide the long brass tubing over the inductor and use room-temperature conducting epoxy to attach it to the SMA connector at the end.
12. Slide the brass sleeve over the filter’s outer conductor.
13. Attach the other SMA connector in the same way as the first SMA connector.
14. Pour the iron powder through the 1/8” hole in the outer conductor.
15. Once the assembly is full of powder, slide the sleeve over the 1/8” hole and seal it in place with room-temperature conducting epoxy.

Figure 3.24: Filter with SMA connectors for tunneling line

3.5 Filter Housing

To prevent EMI from re-entering the wires after they've been filtered, it's crucial to hermetically seal all the conduits and assemblies, as well as shield the filter outputs from the inputs. In order to achieve this, the filters should be housed in an RF-sealed metal assembly with the filters fixed to a metal partition within the housing. The box material and thickness should be such that fields can not significantly penetrate the walls. Three separate housings were made for the three multi-wire ports.

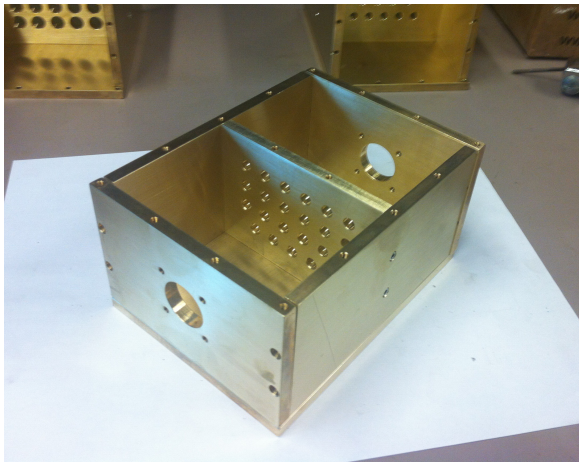

Figure 3.25: Filter housing prior to installing filters, wiring, and connectors

The housing assembly consists of 1/4" brass plates machined on a CNC

milling machine, and fastened together with screws, conductive carbon paste, and silver conductive epoxy.

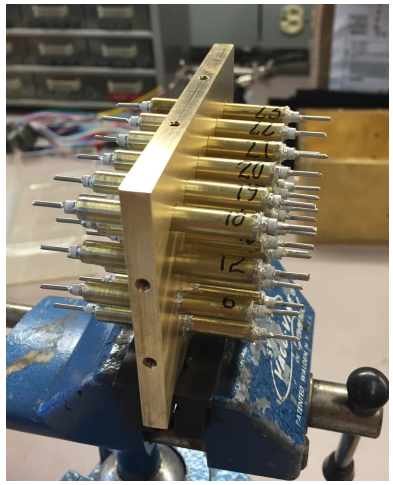

Figure 3.26: Housing partition populated with filters

The filters were sanded-down to fit snugly in the brass partition, and sealed in place with silver conductive epoxy. Once populated, the partition was sealed in the housing with carbon conductive grease.

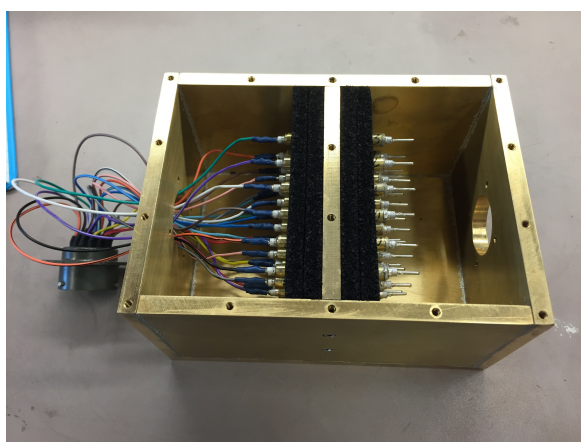

Figure 3.27: Partially assembled filter housing

Before connecting any of the wires to the filters, lossy microwave foam was installed against the housing partition to help attenuate resonances

formed within the partition walls. The foam, manufactured by MAST Technologies (part number MF22-0002-00), is 1/4" thick and has a loss of -21.5 dB at 10 GHz. This alone does not completely damp the resonances present within the housing, however. To further attenuate the resonances, vinyl pouches filled with approximately 75 mL of water are stuffed in the housing. Since water is quite lossy to microwaves, these pouches are very effective at removing resonances.

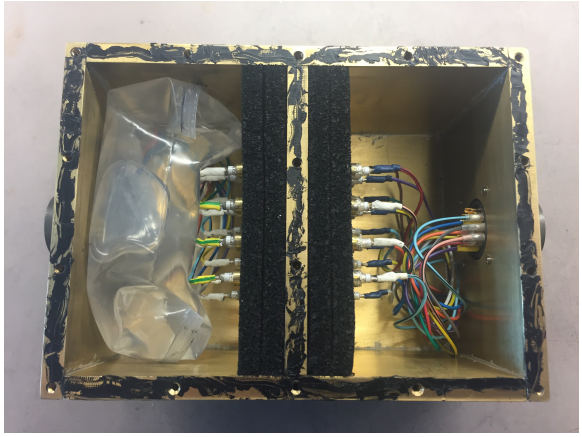

Figure 3.28: Fully populated filter housing

Once all the filters are wired and the lossy foam and water pouch are put in place, the housing lid is sealed to the rest of the housing with a layer of conductive carbon paste.

3.6 Wiring Conduit

In order for the wires connecting the filter housing to the wiring ports on the UHV system to not get re-contaminated with noise, their conduit must be fully shielded. Since the shielding in coaxial cables typically consists of a mesh braid, coaxial cables don't provide adequate shielding at higher frequencies. In order to account for this, the conduit was made of a section of 3/4" rigid bellows with stainless steel adapters to provide the best possible seal to the connectors.

For each conduit end, the strain relief on the collar (Amphenol part no.'s M85049/52-1-16N and M85049/52-1-14N), which allows the conduit connector (Amphenol part no.'s MS3476L14-19P, MS3476L14-19S, MS3476L14-23P and MS3476L14-23S) to be rotated in alignment with the mating con-

nector, was cut and filed off. The newly-filed face of the collar was epoxied to a custom-made adapter which is then slid over and epoxied to the end of the bellows. In this way, the connectors are well-fixed to the bellows and can withstand enough torque to be used without any special concern for breaking the conduit in typical use.

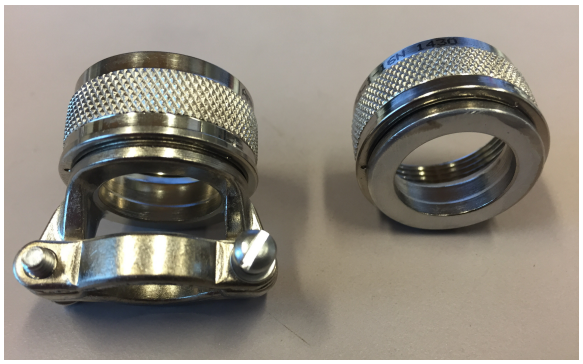

Figure 3.29: Connector collar with strain relief (left) and strain relief removed (right)

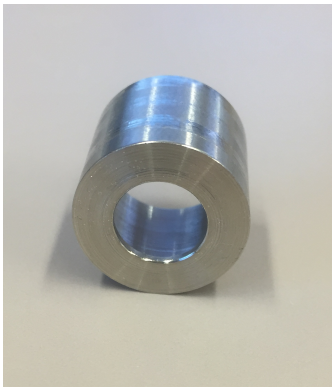

Figure 3.30: Stainless steel piece to connect the filed collars to the bellows

Figure 3.31: Conduit connector, collar, adapter, and bellows epoxied together

Figure 3.32: Wiring conduit

Chapter 4

Attenuation

4.1 Measurement Setup

Attenuation data between 10 MHz and 43.5 GHz were collected on an Agilent N5244A PNA-X Network Analyzer. Since the filters don't have any connectors on them, they were mounted in the same assemblies as the ones connected to the STM connector ports, the only difference being the partition within the housing having a single hole for a filter. This housing also includes the lossy microwave foam and pouches of water to dissipate resonances from within the housing.

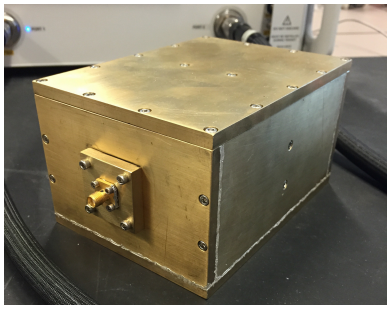

Figure 4.1: Housing with SMA connectors installed to measure filter attenuation on the vector network analyzer

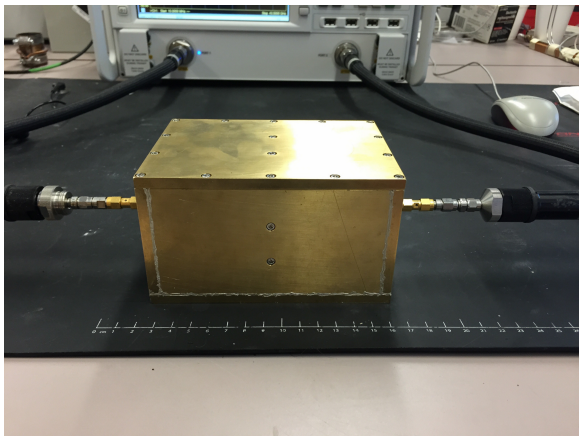

Figure 4.2: Housing connected to vector network analyzer

4.2 Filter Attenuation Characteristics

Due to the relatively high resistivity and low magnetic permeability, stainless steel powder has been an ideal candidate for some powder filters. Though, as mentioned earlier in this thesis, in choosing between stainless steel powder and iron powder, there is a trade-off: steel is an order of magnitude more resistive than iron and so is better at dissipating RF power via the skin effect, but iron has a high magnetic permeability and thus increases the inductance of the filter; which has better attenuation depends on the filter geometry.

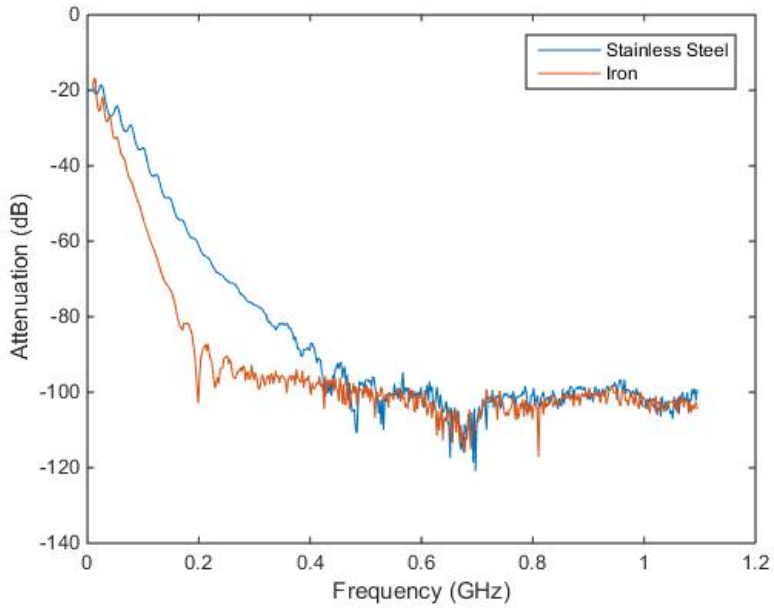

Figure 4.3: Attenuation for stainless steel vs. iron powder LC-Π filters

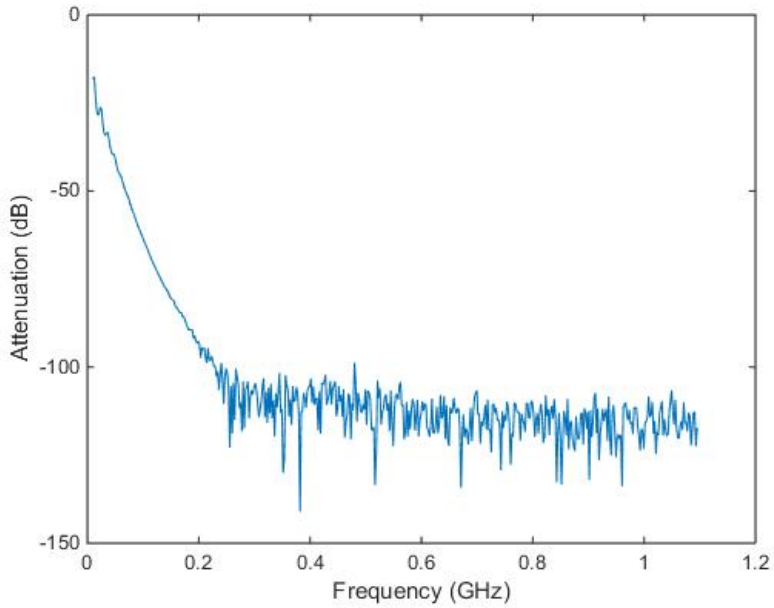

Figure 4.4: Attenuation for tunneling line filter

As shown in Figure 4.3, the roll-off for the iron powder filter attenuation is slightly steeper than that of the stainless steel powder filters, and reaches the noise floor around 200 MHz instead of 500 MHz. The -3 dB point of the iron powder filter was measured to be approximately 1 MHz (The tunneling line filter (Figure 4.4) is essentially the same as the iron powder LC-Π filter, but has SMA connector directly attached). In this geometry, the effect of the increased inductance with iron is stronger than the effect of increased resistance with steel. However, in the geometry of the coarse approach filters, this does not seem to be the case.

Adding iron powder to the filters scales the inductance by the powder's permeability, and since the inductance in the coarse approach filters have about 10 times fewer windings (and thus 10 times lower the inductance) than the LC-Π filters, the absolute value of the increased inductance when using iron instead of stainless steel in the coarse approach filters is much smaller than the improvement in the LC-Π filters. As seen in Figure 4.4, the increased attenuation resulting from this increased inductance is on the same order as the increased attenuation due to the increased RF power dissipated in the more resistive stainless steel powder.

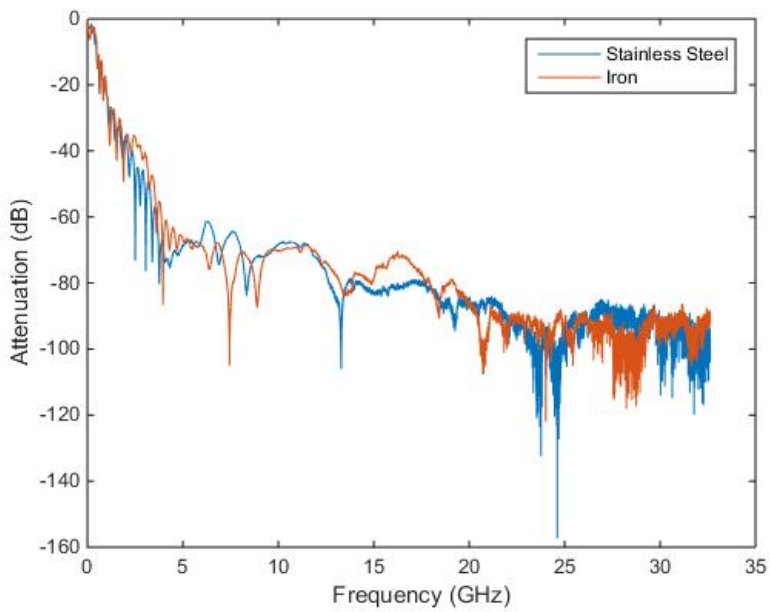

Figure 4.5: Attenuation for stainless steel vs. iron coarse approach filters

The cold bias line filter behaves very similarly to the coarse approach filters. This might be surprising because the cold bias line filter has practically the same inductor as the LC-Π stainless steel powder filters, which has a much greater inductance (and resistance) than the coarse approach filters. This suggests that installing capacitors in the Π configuration plays a very significant role in lowing the cutoff frequency. This was also seen by Lukashenko and Ustinov where the attenuation reached the noise floor (-100 dB) an order of magnitude higher (1 GHz) without capacitors [5].

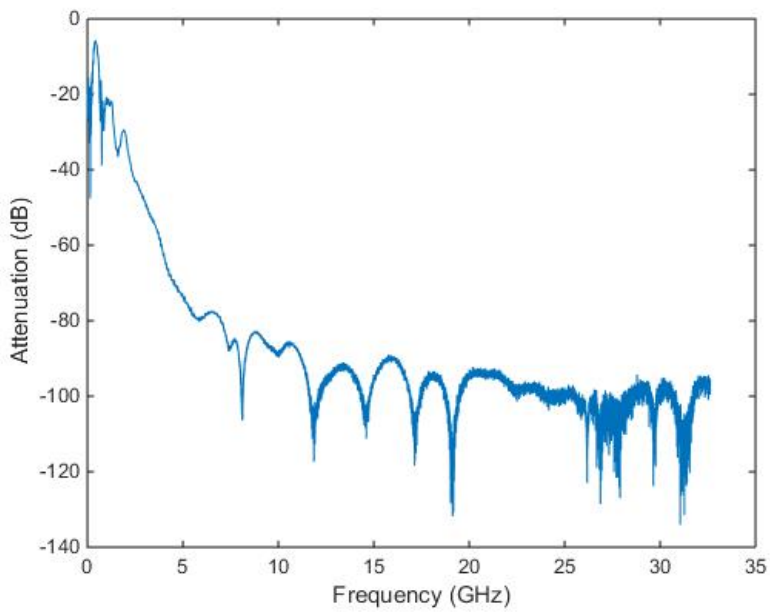

Figure 4.6: Attenuation of cold bias filter, taken at room temperature

It's worth comparing these characteristics to other filters in the literature. The powder filters made by Lukashenko and Ustinov [5] perform slightly better than the LC-Π filters in this thesis, even though they use stainless steel powder instead of iron. Whereas the stainless steel LC-Π filters in this thesis reach -100 dB around 400 MHz, Lukashenko's stainless steel filters do this around 200 MHz. The improved performance of the Lukashenko and Ustinov filters is likely due to the fact they use 4 nF capacitors instead of 100 pF.

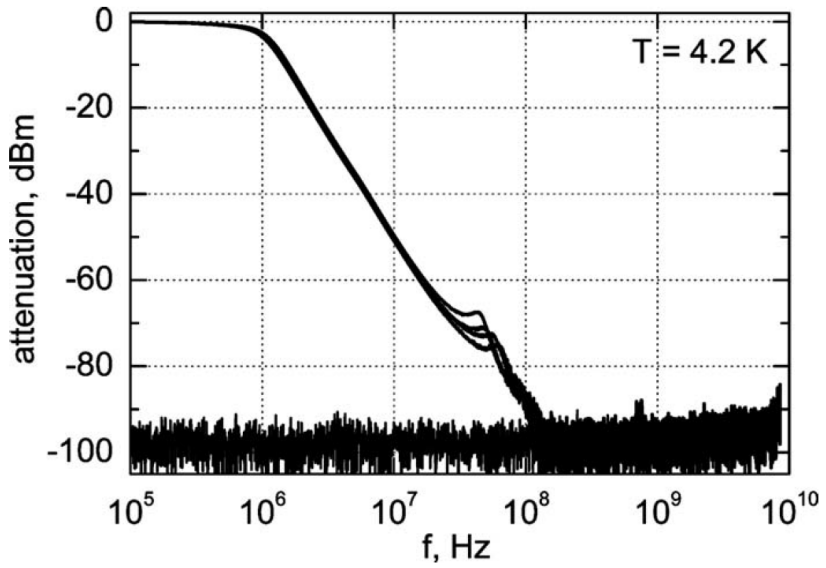

Figure 4.7: Attenuation of Lukashenko LC-Π powder filters [5]

At the time of this writing, it seems this LC-Π powder filter design has the best performance out of filters used in low temperature physics experiments. Other filters have higher cutoff frequencies, but may be more desirable because they are more easily manufactured. For instance, the microfabricated meander line surrounded with stainless steel powder designed by Hélène le Sueur and Philippe Joyez reaches -100 dB around 4.5 GHz, but can be fabricated much more easily [2].

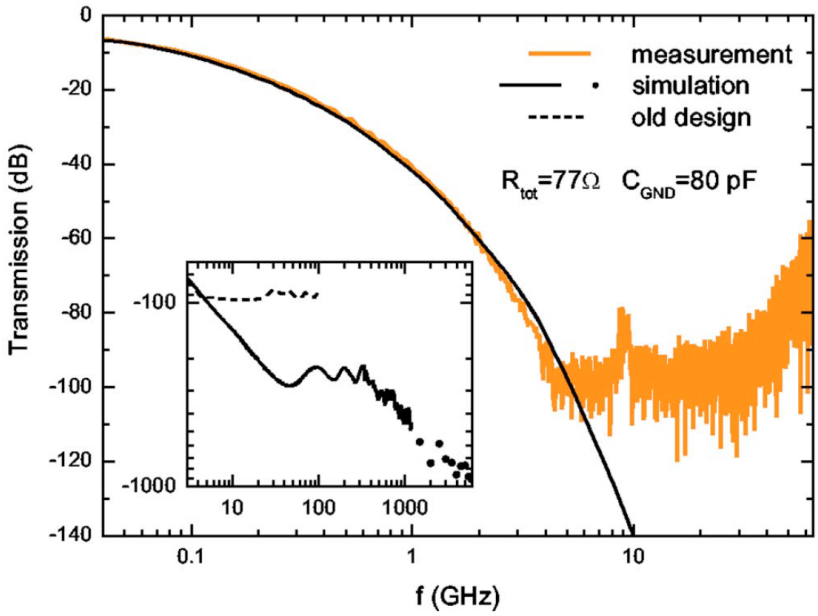

Figure 4.8: Attenuation of microfabricated le Sueur meander line powder filters [2]

Chapter 5

Conclusion

Low temperature physics experiments rely on very low noise systems to meet scientific standards. Scanning tunneling spectroscopy (STS) measurements aim to resolve features in the local density of states (LDOS), which are on the order of 10 μeV, requiring experimental temperatures to be extremely low.

The dilution refrigeration scanning tunneling microscope (STM) at the UBC Laboratory for Atomic Imaging Research (LAIR) is capable of reaching temperatures below 100 mK. However, ambient radio-frequency noise can enter the system and contaminate the tunneling signal. In doing so, energy resolution in STS measurements is decreased which increases the effective temperature to levels which may obscure certain features in the LDOS. In order to fully exploit the capabilities of the system, a set of microwave filters was built to eliminate electromagnetic interference (EMI) and reduce the effective temperature of our STS measurements.

In this thesis I present a technical description of metal powder filters used to eliminate EMI up to seemingly indefinite frequencies. A brief overview of the LAIR STM instrumentation is given, followed by step-by-step instructions for how to build the different kinds of filters used on this system. Finally, I present attenuation data taken to characterize the filters.

The LC-Π iron powder filters have a cutoff frequency of approximately 1 MHz and reach the noise floor (approx. -100 dB) at 200 MHz. The filters used on the coarse approach lines of the STM and the cold bias filter are built without the use of capacitors and reach -80 dB around 5 GHz.

Bibliography

[1] `http://lair.phas.ubc.ca/facility/`, *retrieved on March 29, 2016.*

[2] H. Le Sueur, P. Joyez, "Microfabricated electromagnetic filters for millikelvin experiments," *Rev. Sci. Instrum.*, vol. 77, no. 11, 2006.

[3] M. Assig, et al., "A 10 mK scanning tunneling microscope operating in ultra high vacuum and high magnetic fields," *Rev. Sci. Instrum.*, vol. 84, no. 3, 2013.

[4] J.M. Martinis, M.H. Devoret, J. Clarke, "Experimental tests for the quantum behavior of a macroscopic degree of freedom: The phase difference across a Josephson junction," *Phys. Rev. B*, vol. 35, no. 10, 1987.

[5] A. Lukashenko, A.V. Ustinov, "Improved powder filters for qubit measurements," *Rev. Sci. Instrum.*, vol. 79, no. 1, 2008.

[6] K. Sapchuk, "Construction and Commissioning of the UBC Ultra High Vacuum Gigahertz 2D Tesla Ultra Low Temperature Scanning Tunneling Microscope," April 2012